Syntheses of the Phenylchalcogenolate Complexes $(\eta^5\text{-}C_5Me_5)_2Zr(EPh)_2$ (E = O, S, Se, Te) and $(\eta^5\text{-}C_5H_5)_2Zr(OPh)_2$: Structural Comparisons within a Series of Complexes Containing Zirconium−Chalcogen Single Bonds

William A. Howard, Tina M. Trnka, and Gerard Parkin*

Department of Chemistry, Columbia University, New York, New York 10027

Received May 19, 1995®

The complete series of phenylchalcogenolate derivatives of permethylzirconocene $Cp^*_2Zr(EPh)_2$ ($Cp^* = \eta^5\text{-}C_5Me_5$; E = O, S, Se, Te) has been prepared by the reactions of $Cp^*_2Zr(CO)_2$ with PhOH and Ph_2E_2 (E = S, Se, Te). The molecular structures of all of the derivatives $Cp^*_2Zr(EPh)_2$ have been determined by X-ray diffraction, thereby providing evidence that the nature of the bonding varies as a function of the chalcogen. Specifically, the structure of the phenoxo derivative is notably distinct from those of its heavier congeners. For example, whereas the Zr−S, Zr−Se, and Zr−Te bond lengths are comparable to the sum of their respective covalent radii, the Zr−O bond length is significantly shorter than the sum of the covalent radii, as would be anticipated due to an increased ionic contribution to the bonding. In addition, the Zr−O−C bond angle [172.7(2)°] in $Cp^*_2Zr(OPh)_2$ is effectively linear, whereas the Zr−E−C bond angles for the heavier congeners are significantly bent [113°−119°]. Comparison of the structure of $Cp^*_2Zr(OPh)_2$ with that of the less substituted zirconocene derivative $Cp_2Zr(OPh)_2$, which possesses a bent Zr−O−C moiety [147(1)°], suggests that the linearity of $Cp^*_2Zr(OPh)_2$ may be attributed to steric factors. Thus, short M−OR bond lengths and linear M−O−R angles are not necessarily a consequence of strong $p\pi - d\pi$ lone pair donation from oxygen to the metal. $Cp^*_2Zr(OPh)_2$ is monoclinic: $C2/c$ (No. 15), a = 11.049(2) Å, b = 15.445(3) Å, c = 17.141(3) Å, β = 104.24(1)°, and Z = 4. $Cp^*_2Zr(SPh)_2$ is monoclinic: $C2/c$ (No. 15), a = 14.444(4) Å, b = 11.449(2) Å, c = 18.262(3) Å, β = 103.39(2)°, and Z = 4. $Cp^*_2Zr(SePh)_2$ is hexagonal: $P6_1$ (No. 169), a = 12.903(2) Å, c = 31.923(6) Å, and Z = 6. $Cp^*_2Zr(TePh)_2$ is monoclinic: $P2_1/c$ (No. 14), a = 16.917(3) Å, b = 25.326(6) Å, c = 15.234(4) Å, β = 107.95(2)°, and Z = 8. $Cp_2Zr(OPh)_2$ is orthorhombic: $Aba2$ (No. 41), a = 8.274(3) Å, b = 19.843(9) Å, c = 11.586(8) Å, and Z = 4.

Introduction

As part of our recent investigations of multiple bonding between transition metals and chalcogens,[1−4] we have determined the molecular structures of two complete series of terminal chalcogenido complexes, namely, the zirconium and hafnium derivatives $Cp^{Et*}_2M(E)(NC_5H_5)$ ($Cp^{Et*} = \eta^5\text{-}C_5Me_4Et$; M = Zr,[2b] Hf;[2c] E = O, S, Se, Te). These studies have allowed differences in the nature of the multiple bonds in these systems to be elucidated; for example, whereas the zirconium−sulfido, −selenido, and −tellurido interactions may be reasonably described as Zr=E covalent double bonds, the zirconium−oxo interaction possesses substantial ionic character *via* the resonance structure $Zr^+{-}O^-$.[2b] For purposes of comparison with these studies on Zr=E multiple bonding, we have sought to determine the structures of related complexes containing formal single Zr−E bonds (E = O, S, Se, Te). Therefore, in this paper we describe the complete series of structures of the permethylzirconocene complexes $Cp^*_2Zr(EPh)_2$ (E = O, S, Se, Te), focusing particular attention on the metrical details associated with the [Zr−E−Ph] moiety. Additional comparison of the structure of the phenoxo complex $Cp^*_2Zr(OPh)_2$ with that of its unsubstituted zirconocene analogue $Cp_2Zr(OPh)_2$ also allows the influence of steric effects on the bonding of the [Zr−O−Ph] moiety to be identified.

Results and Discussion

We have recently reported the syntheses of a series of complexes which contain formal Zr−E single bonds, namely, the hydrochalcogenido derivatives $Cp^*_2Zr(EH)[\eta^1\text{-}OC(Ph){=}CH_2]$ (E = O, S, Se, Te).[2b] The hydroxo, hydrosulfido, and hydroselenido derivatives were structurally characterized by X-ray diffraction, but attempts to determine the structure of the hydrotellurido analogue $Cp^*_2Zr(TeH)[\eta^1\text{-}OC(Ph){=}CH_2]$ were thwarted by its limited stability in solution, thereby preventing the formation of crystals suitable for X-ray diffraction analysis. For this reason, we have synthesized another series of more stable permethylzirconocene complexes with zirconium−chalcogen single bonds, namely the phenylchalcogenolate derivatives $Cp^*_2Zr(EPh)_2$ (E = O, S, Se, Te),[5] in order to furnish comparisons between zirconium−chalcogen single and multiple bonds in two closely related systems.

1. Syntheses of $Cp^*_2Zr(EPh)_2$ (E = O, S, Se, Te) and $Cp_2Zr(OPh)_2$. The series of permethylzirconocene phenylchalcogenolate complexes $Cp^*_2Zr(EPh)_2$ (E = O,[6] S, Se, Te)

® Abstract published in *Advance ACS Abstracts,* October 15, 1995.

(1) (a) Rabinovich, D.; Parkin, G. *J. Am. Chem. Soc.* **1991**, *113*, 5904−5905. (b) Rabinovich, D.; Parkin, G. *J. Am. Chem. Soc.* **1991**, *113*, 9421−9422. (c) Rabinovich, D.; Parkin, G. *J. Am. Chem. Soc.* **1993**, *115*, 9822−9823. (d) Rabinovich, D.; Parkin, G. *Inorg. Chem.* **1994**, *33*, 2313−2314. (e) Murphy, V. J.; Parkin, G. *J. Am. Chem. Soc.* **1995**, *117*, 3522−3528.

(2) (a) Howard, W. A.; Waters, M.; Parkin, G. *J. Am. Chem. Soc.* **1993**, *115*, 4917−4918. (b) Howard, W. A.; Parkin, G. *J. Am. Chem. Soc.* **1994**, *116*, 606−615. (c) Howard, W. A.; Parkin, G. *J. Organomet. Chem.* **1994**, *472*, C1−C4. (d) Howard, W. A.; Trnka, T. M.; Parkin, G. *Organometallics* **1995**, *14*, 4037−4039.

(3) (a) Shin, J. H.; Parkin, G. *Organometallics* **1994**, *13*, 2147−2149. (b) Shin, J. H.; Parkin, G. *Organometallics* **1995**, 14, 1104−1106.

(4) For related studies on multiple bonding between main group metals and the chalcogens, see: (a) Kuchta, M. C.; Parkin, G. *J. Chem. Soc., Chem. Commun.* **1994**, 1351−1352. (b) Kuchta, M. C.; Parkin, G. *J. Am. Chem. Soc.* **1994**, *116*, 8372−8373.

(5) For a review that includes a discussion of zirconocene−chalcogenolate complexes, see: Hey-Hawkins, E. *Chem. Rev.* **1994**, *94*, 1661−1717.

0020-1669/95/1334-5900$09.00/0

Scheme 1

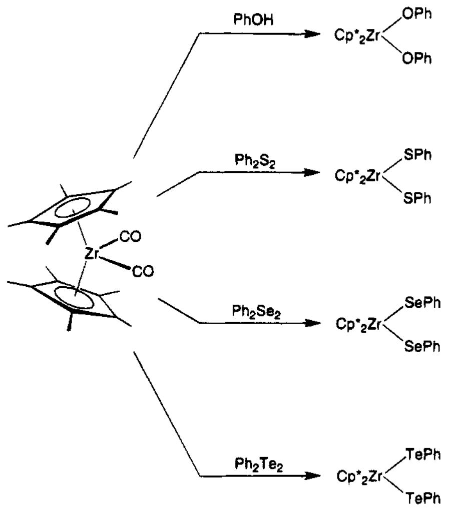

is conveniently obtained by the reactions of the dicarbonyl $Cp^*_2Zr(CO)_2$ with PhOH and Ph_2E_2 (E = S, Se, Te), as illustrated in Scheme 1. The use of R_2E_2 as reagents for the syntheses of organochalcogenolate derivatives is well established;[7] for example, the reactions between $Cp_2Zr(CO)_2$ and R_2S_2 have been employed previously in the syntheses of the thiolate complexes $Cp_2Zr(SR)_2$ (R = Ph, Et).[8] In addition to $Cp_2Zr(SPh)_2$, the other previously reported zirconocene analogues $Cp_2Zr(EPh)_2$ (E = O, Se, Te)[9,10] may also be synthesized by the analogous reactions of $Cp_2Zr(CO)_2$ with PhOH and Ph_2E_2 (E = Se, Te). The phenoxo derivative $Cp_2Zr(OPh)_2$ may also be prepared by the reaction of Cp_2ZrMe_2 with PhOH.

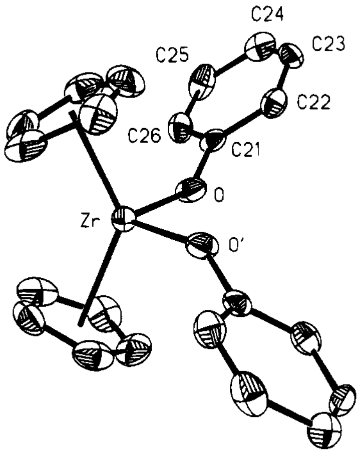

Figure 1. Molecular structure of $Cp_2Zr(OPh)_2$.

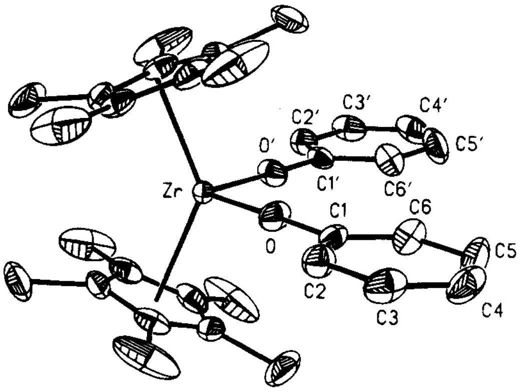

Figure 2. Molecular structure of $Cp^*_2Zr(OPh)_2$.

The phenylselenolate and phenyltellurolate complexes $Cp^*_2Zr(SePh)_2$ and $Cp^*_2Zr(TePh)_2$ are characterized by ^{77}Se and ^{125}Te NMR signals at δ 710 and 1004 ppm, respectively, *i.e.*, shifted slightly downfield from their cyclopentadienyl counterparts, $Cp_2Zr(SePh)_2$ (δ 686 ppm) and $Cp_2Zr(TePh)_2$ (δ 982 ppm).[11] For reference, similar ^{77}Se NMR chemical shifts in the range δ 664−694 ppm have been observed for $(\eta^5\text{-}C_5H_4R')_2Zr(SeR)_2$ derivatives (R' = H, Bu^t; R = Ph, *p*-Tol).[12] Although we are not aware of ^{125}Te NMR studies on related organotellurolate−zirconocene complexes, ^{125}Te NMR data have been reported recently for some silyltellurolate−zirconocene complexes, demonstrating a very large ^{125}Te NMR chemical shift range for such moieties: $Cp_2Zr[TeSi(SiMe_3)_3]_2$ (δ −26 ppm),[13] $Cp_2Zr[TeSi(SiMe_3)_3]Me$ (δ −207 ppm),[13] $Cp_2Zr[TeSi(SiMe_3)_3](\eta^2\text{-}COMe)$ (δ −1146 ppm),[13] $Cp_2Zr(TeSiPh_3)_2$ (δ 15 ppm),[14] and $(\eta^5\text{-}C_5H_4Bu^t)_2Zr(TeSiPh_3)_2$ (δ 75 ppm).[14]

2. Structures of $Cp^*_2Zr(EPh)_2$ (E = O, S, Se, Te) and $Cp_2Zr(OPh)_2$. The molecular structures of $Cp_2Zr(OPh)_2$ and $Cp^*_2Zr(EPh)_2$ (E = O, S, Se, Te) have been determined by X-ray diffraction, as illustrated in Figures 1−5. Selected metrical data for these complexes are summarized in Table 1.

---

(6) The phenoxo derivative $Cp^*_2Zr(OPh)_2$ has been previously synthesized by the reaction of $Cp^*_2ZrMe_2$ with PhOH. See: Schock, L. E.; Marks, T. J. *J. Am. Chem. Soc.* **1988**, *110*, 7701−7715.

(7) Examples of oxidations of low valent metal centers with R_2E_2 reagents (E = S, Se, Te) are abundant. See, for example: (a) Lang, R. F.; Ju, T. D.; Kiss, G.; Hoff, C. D.; Bryan, J. C.; Kubas, G. J. *J. Am. Chem. Soc.* **1994**, *116*, 7917−7918. (b) Lang, R. F.; Ju, T. D.; Kiss, G.; Hoff, C. D.; Bryan, J. C.; Kubas, G. J. *Inorg. Chem.* **1994**, *33*, 3899−3907. (c) Goh, L. Y.; Tay, M. S.; Wei, C. *Organometallics* **1994**, *13*, 1813−1820. (d) Liaw, W.-F.; Ou, D.-S.; Horng, Y.-C.; Lai, C.-H.; Lee, G.-H.; Peng, S.-M. *Inorg. Chem.* **1994**, *33*, 2495−2496. (e) Liaw, W.-F.; Chiang, M.-H.; Liu, C.-J.; Harn, P.-J.; Liu, L.-K. *Inorg. Chem.* **1993**, *32*, 1536−1538. (f) Liaw, W.-F.; Lai, C.-H.; Lee, C.-K.; Lee, G.-H.; Peng, S.-M. *J. Chem. Soc., Dalton Trans.* **1993**, 2421−2422. (g) Liaw, W.-F.; Lai, C.-H.; Chiang, M.-H.; Hsieh, C.-K.; Lee, G.-H.; Peng, S.-M. *J. Chin. Chem. Soc.* **1993**, *40*, 437−444. (h) Aye, K.-T.; Vittal, J. J.; Puddephatt, R. J. *J. Chem. Soc., Dalton Trans.* **1993**, 1835−1839. (i) Andreu, P. L.; Cabeza, J. A.; Miguel, D.; Riera, V.; Villa, M. A.; Garcia-Granda, S. *J. Chem. Soc., Dalton Trans.* **1991**, 533−536. (j) Canich, J. A. M.; Cotton, F. A.; Dunbar, K. R.; Falvello, L. R. *Inorg. Chem.* **1988**, *27*, 804−811. (k) Cotton, F. A.; Dunbar, K. R. *Inorg. Chem.* **1987**, *26*, 1305−1309. (l) Liaw, W.-F.; Ou, D.-S.; Li, Y.-S.; Lee, W.-Z.; Chuang, C.-Y.; Lee, Y.-P.; Lee, G.-H.; Peng, S.-M. *Inorg. Chem.* **1995**, *34*, 3747−3754. (m) Brennan, J. G.; Siegrist, T.; Carroll, P. J.; Stuczynski, S. M.; Reynders, P.; Brus, L. E.; Steigerwald, M. L. *Chem. Mater.* **1990**, *2*, 403−409.

(8) Fochi, G.; Guidi, G.; Floriani, C. *J. Chem. Soc., Dalton Trans.* **1984**, 1253−1256.

(9) The complexes $Cp_2Zr(EPh)_2$ (E = O, S, Se, Te) have been previously reported. For example, $Cp_2Zr(OPh)_2$ has been synthesized by the reactions of Cp_2ZrX_2 (X = Cl,[9a] Br[9b]) with PhOH in the presence of Et_3N; $Cp_2Zr(SPh)_2$ has been prepared by the reaction of Cp_2ZrCl_2 with PhSH in the presence of Et_3N;[9c] $Cp_2Zr(SePh)_2$ has been prepared by the reaction of Cp_2ZrCl_2 with PhSeH in the presence of Et_3N,[9c] and by the reaction of Cp_2ZrCl_2 with PhSeLi;[9d] and $Cp_2Zr(TePh)_2$ has been prepared by the reaction of Cp_2ZrCl_2 with PhTeLi.[9d] (a) Shoushan, C.; Yiyin, L.; Jitao, W. *Sci. Sin., Ser. B* **1982**, *25*, 227−235. (b) Andrä, K.; Hille, E. *Z. Chem.* **1968**, *8*, 65−66. (c) Köpf, H. *J. Organomet. Chem.* **1968**, *14*, 353−358. (d) Sato, M.; Yoshida, T. *J. Organomet. Chem.* **1974**, *67*, 395−399.

(10) A related series of isostructural zirconium−chalcogenolate complexes includes $Cp_2Zr(EMe)_2$ (E = O,[10a] S,[10b] Se,[10c,d] Te[10b]). (a) Gray, D. R.; Brubaker, C. H., Jr. *Inorg. Chem.* **1971**, *10*, 2143−2146. (b) Tainturier, G.; Fahim, M.; Trouvé-Bellan, G.; Gautheron, B. *J. Organomet. Chem.* **1989**, *376*, 321−332. (c) Gautheron, B.; Tainturier, G.; Meunier, Ph. *J. Organomet. Chem.* **1981**, *209*, C49−C51. (d) Tainturier, G.; Gautheron, B.; Pouly, S. *Nouv. J. Chim.* **1986**, *10*, 625−630.

(11) The relationship between the ^{77}Se and ^{125}Te NMR data for $Cp^*_2Zr(EPh)_2$ and $Cp_2Zr(EPh)_2$ (E = Se, Te) is in agreement with the correlation between the chemical shifts of a series of terminal selenido and tellurido complexes. Rabinovich, D.; Parkin, G. *Inorg. Chem.*, in press.

(12) Granger, P.; Gautheron, B.; Tainturier, G.; Pouly, S. *Org. Magn. Reson.* **1984**, *22*, 701−704.

(13) Christou, V.; Wuller, S. P.; Arnold, J. *J. Am. Chem. Soc.* **1993**, *115*, 10545−10552.

(14) Gindelberger, D. E.; Arnold, J. *Organometallics* **1994**, *13*, 4462−4468.

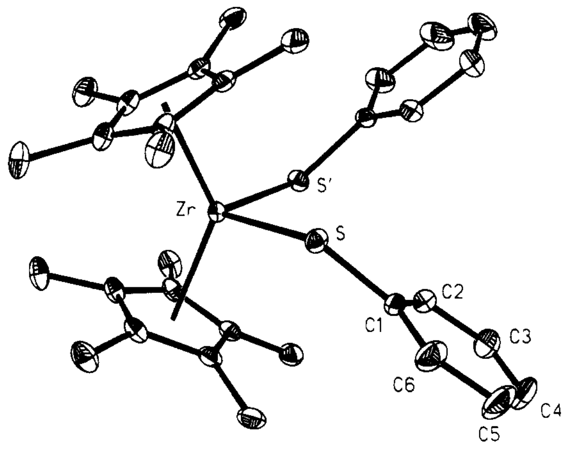

Figure 3. Molecular structure of Cp*$_2$Zr(SPh)$_2$.

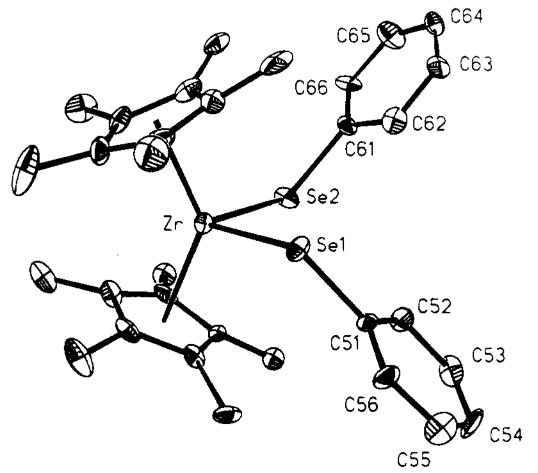

Figure 4. Molecular structure of Cp*$_2$Zr(SePh)$_2$.

For the heavier chalcogens (S, Se, Te), the Zr—E bond lengths are close to the sum of the respective single bond covalent radii and are comparable to the average values observed in other complexes (Table 2). In contrast, however, the Zr—O bond length in Cp*$_2$Zr(OPh)$_2$ is *ca.* 0.17 Å shorter than the sum of the covalent bond radii for zirconium and oxygen. A similar observation was made previously for the hydroxo—enolate complex Cp*$_2$Zr(OH)[η^1-OC(Ph)=CH$_2$], in which the zirconium—oxygen bonds [2.010(2) and 1.993(2) Å] are also shorter than the sum of the covalent bond radii.[2b] Although such a shortening of the Zr—O bond with respect to the sum of the covalent radii may be attributed to enhanced π-bonding, it is rather believed to be a consequence of partial ionic character in the zirconium—oxygen bond (*i.e.*, Zr$^{\delta+}$—O$^{\delta-}$). An ionic contribution would be expected to be most pronounced for the Zr—O derivative due to (i) the greater electronegativity of oxygen with respect to the other chalcogens (*cf.* the Schomaker—Stevenson equation)[15] and (ii) the smaller size of oxygen, both of which serve to increase the Coulombic stabilization associated with the dipolar moiety Zr$^{\delta+}$—O$^{\delta-}$. Moreover, the shortness of the Zr=O bond in the terminal oxo complex Cp$^{\text{Et}}$*$_2$Zr(O)(NC$_5$H$_5$) has also been rationalized in terms of an ionic contribution *via* the resonance structure Zr$^+$—O$^-$, a suggestion that is well-supported by Cundari's computational studies.[16] Specifically, Cundari has identified that the electron density constituting the Zr=E π-bond is significantly more localized on oxygen than for the other chalcogens, so that there is a fundamental difference between the Zr=O and Zr=E (E = S, Se, Te) bonds. By analogy, the shortness of the Zr—OPh bond in Cp*$_2$Zr(OPh)$_2$ is not necessarily a consequence of enhanced oxygen-to-zirconium pπ—dπ bonding (*vide infra*).[17]

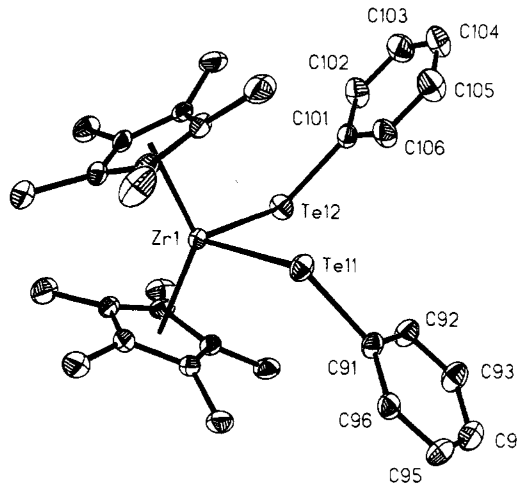

Figure 5. Molecular structure of Cp*$_2$Zr(TePh)$_2$ (only one of the independent molecules is shown).

Perhaps the most striking difference in the structures of the phenylchalcogenolate complexes Cp*$_2$Zr(EPh)$_2$ is the near linearity of Zr—O—Ph *vs* the significantly bent Zr—E—Ph (E = S, Se, Te) moieties (Table 1). Thus, the Zr—E—C bond angle experiences a substantial decrease from 172.7(2)° in Cp*$_2$Zr(OPh)$_2$ to 119.0(1)° in Cp*$_2$Zr(SPh)$_2$. In this regard, the changes in Zr—E—Ph bond angles follow the trend observed for both H$_2$E [H$_2$O (104.5°), H$_2$S (92.2°), H$_2$Se (91.0°), H$_2$Te (89.5°)][18-20] and R$_2$E,[21] although the change in the Zr—E—Ph bond angle of 53.7° between Cp*$_2$Zr(OPh)$_2$ and Cp*$_2$Zr(SPh)$_2$ is certainly much greater than those observed for both H$_2$E (12.3°) and R$_2$E (13.6°).[22,23] In contrast to the large change in the Zr—E—C bond angle from Cp*$_2$Zr(OPh)$_2$ to Cp*$_2$Zr(TePh)$_2$, there is relatively little perturbation in E—Zr—E bond angles (*ca.* 97°—101°).

For comparison purposes, Zr—O bond length and Zr—O—C bond angle data for a selection of zirconocene derivatives are summarized in Table 3 and Figure 6. Evidently, there exists no correlation between the Zr—O bond length and the Zr—O—C

---

(15) The empirical Schomaker—Stevenson equation[15a] would predict a shortening of *ca.* 0.2 Å for a Zr—O bond due to a polar contribution. However, it should be noted that modifications[15b,c] and criticisms[16d,e] of the Schomaker—Stevenson equation have also been presented. (a) Schomaker, V.; Stevenson, D. P. *J. Am. Chem. Soc.* **1941**, *63*, 37—40. (b) Pauling, L. *The Nature of the Chemical Bond*, 3rd ed.; Cornell University Press: Ithaca, NY, 1960. (c) Blom, R.; Haaland, A. *J. Mol. Struct.* **1985**, *128*, 21—27. (d) Wells, A. F. *J. Chem. Soc.* **1949**, 55—67. (e) Wells, A. F. *Structural Inorganic Chemistry*, 5th ed.; Oxford University Press: Oxford, U.K., 1984; pp 287—291.

(16) (a) Benson, M. T.; Cundari, T. R.; Lim, S. J.; Nguyen, H. D.; Pierce-Beaver, K. *J. Am. Chem. Soc.* **1994**, 116, 3955—3966. (b) Benson, M. T.; Cundari, T. R.; Li, Y.; Strohecker, L. A. *Int. J. Quantum Chem.: Quantum Chem. Symp.* **1994**, *28*, 181—194.

(17) Power has also concluded that the short Al—O and Ga—O bond lengths in (Bu^t)$_2$MOAr complexes is a manifestation of an ionic contribution and is not a consequence of a π-donation from O to M. See: Petrie, M. A.; Olmstead, M. M.; Power, P. P. *J. Am. Chem. Soc.* **1991**, *113*, 8704—8708.

(18) Gillespie, R. J. *J. Am. Chem. Soc.* **1960**, *82*, 5978—5983.

(19) The larger bond angle in H$_2$O, compared to the almost 90° bond angles in H$_2$S, H$_2$Se, and H$_2$Te, is commonly associated with the increased tendency of oxygen to participate in hybridization in order to minimize the Pauli repulsion between the two O—H bonds. Since Pauli repulsion decreases exponentially with distance, it is less significant for the heavier congeners with longer E—H bond lengths. Thus, the bonding in H$_2$E (E = S, Se, Te) is predominantly derived by interactions of the hydrogen 1s orbital with those of the chalcogen np orbitals, with little contribution from interaction with the chalcogen ns orbital. See: Kutzelnigg, W. *Angew. Chem., Int. Ed. Engl.* **1984**, *23*, 272—295.

(20) For a recent discussion of relativistic effects on H$_2$E, see: Pisani, L.; Clementi, E. *J. Chem. Phys.* **1994**, *101*, 3079—3084.

(21) For example, a search of the Cambridge Structural Database (updated March 1994) indicates that the mean C—O—C bond angle (111.3°) is substantially larger than the mean C—S—C bond angle (97.7°).

Table 1. Selected Bond Lengths (Å) and Angles (deg) for $Cp_2Zr(OPh)_2$ and $Cp^*_2Zr(EPh)_2$

	$Cp_2Zr(OPh)_2$	$Cp^*_2Zr(OPh)_2$	$Cp^*_2Zr(SePh)_2$	$Cp^*_2Zr(SePh)_2$	$Cp^*_2Zr(TePh)_2$[a]
$Zr-E_{av}$	2.008(14)	1.989(3)	2.522(1)	2.651[3]	2.87[2]
$E-C_{av}$	1.321(18)	1.333(4)	1.774(3)	1.93[2]	2.12[2]
$Zr-C_{av}$	2.52[5]	2.56[2]	2.57[4]	2.58[7]	2.56[5]
E−Zr−E	98.1(9)	99.4(1)	100.9(1)	99.5(1)	97.2[1]
Zr−E−C	146.7(11)	172.7(2)	119.0(1)	117.3[5]	113.1[7]

[a] Average values for two independent molecules.

Table 2. Comparison of Zr−E Bond Lengths

	$d(Zr-E_{av})$[a]/Å	Σr_{cov}[b]/Å	$d(Zr-E_{av})$ for $Cp^*_2Zr(EPh)_2$/Å
O	2.18	2.16	1.989(3)
S	2.59	2.54	2.522(1)
Se	2.65	2.67	2.651[3]
Te	2.83	2.87	2.87[2]

[a] Data taken from a search of the Cambridge Structural Database which did not distinguish between normal covalent and dative covalent bonds. [b] Covalent radii: Zr (1.50 Å), O (0.66 Å), S (1.04 Å), Se (1.17 Å), Te (1.37 Å). Data taken from ref 15b, p 224, with the exception of zirconium for which the estimate was taken from data provided in ref 2b.

Table 3. Metrical Data for Aryloxy and Alkoxy Zirconocene Derivatives

	d(Zr−O)/Å	Zr−O−C/deg	ref
$Cp^*_2Zr(OPh)_2$	1.989(3)	172.7(2)	this work
$Cp_2Zr(OPh)_2$	2.01(1)	147(1)	this work
$Cp_2Zr(OC_6F_5)_2$	1.991(2)	163.7(2)	*c*
$(\eta^5\text{-}C_5H_4Me)_2Zr(OC_6H_3Cl_2)_2$	2.03[1]	148[1]	*d*
$Cp_2Zr(OAr)(\eta^2\text{-}Bu^tNCCH_2Ph)$[a]	2.079(3)	154.8(3)	*e*
$Cp_2Zr(OAr)(CH_2Ph)$[b]	1.981(6)	165.3(5)	*e*
$Cp_2Zr[O(\eta\text{-}Ph)Cr(CO)_3]_2$	1.992(6)	153.6(6)	*f*
$Cp_2Zr[OCH_2(\eta\text{-}Ph)Cr(CO)_3]_2$	1.956(2) 1.948(2)	155.9(2) 157.9(3)	*g*
$Cp_2Zr(OPh)(\eta^2\text{-}S_2CNMe_2)$	2.023(8)	159.7(8)	*h*
$Cp_2Zr[\eta^1\text{-}OC(CH_2)PPh_2]Cl$	1.960(3)	163.6(3)	*i*
$Cp_2Zr[\eta^1\text{-}OC(CH_2)NPh_2]Cl$	1.976(3)	147.3(3)	*j*
$Cp_2Zr(OC_6H_4PPh_2)Cl$	1.993(6)	144.3(3)	*k*
$Cp_2Zr(OC_6H_4PPh_2)_2$	1.979(7) 2.004(1)	160.2(5) 144.3(3)	*k*
$[Cp_2Zr(OPh)]_2O$	2.073(7)	153.0(6)	*l*
$[Cp_2Zr(OC_6H_4Cl)]_2O$	1.99(2) 2.00(2)	177(2) 153(2)	*m*
$Cp_2Zr[\eta^1\text{-}OC(Me)CPh_2]Me$	1.975(3)	150.8(3)	*n*
$Cp_2Zr[\eta^1\text{-}OC(Me)CPh_2]_2$	2.004(6) 1.999(6) 1.989(7) 1.993(7)	144.2(5) 148.6(5) 143.5(6) 153.8(5)	*n*
$Cp_2Zr[\eta^1\text{-}OC(TMS)CH(anthryl)]Cl$	1.950(4)	157.7(3)	*o*

[a] Ar = $2\text{-Me-6-}Bu^tC_6H_3$. [b] Ar = $2,4\text{-}Me_2\text{-6-cyMe}C_6H_2$. [c] Amor, J. I.; Burton, N. C.; Cuenca, T.; Gómez-Sal, P.; Royo, P. *J. Organomet. Chem.* **1995**, *485*, 153−160. [d] Jinbi, D.; Meizhen, L.; Jiping, Z.; Shoushen, C. *J. Struct. Chem.* **1982**, *1*, 63−69. [e] Steffey, B. D.; Truong, N.; Chebi, D. E.; Kerschner, J. L.; Fanwick, P. E.; Rothwell, I. P. *Polyhedron* **1990**, *9*, 839−845. [f] Heppert, J. A.; Boyle, T. J.; Takusagawa, F. *Organometallics* **1989**, *8*, 461−467. [g] Gau, H.-M.; Chen, C.-T.; Schei, C.-C. *J. Organomet. Chem.* **1992**, *424*, 307−317. [h] Femec, D. A.; Groy, T. L.; Fay, R. C. *Acta. Crystallogr.* **1991**, *C47*, 1811−1814. [i] Veya, P.; Floriani, C.; Chiesi-Villa, A.; Guastini, C. *Organometallics* **1991**, *10*, 2991−2993. [j] Veya, P.; Floriani, C.; Chiesi-Villa, A.; Guastini, C. *J. Chem. Soc., Chem. Commun.* **1991**, 1166−1167. [k] Miquel, L.; Basso-Bert, M.; Choukroun, R.; Madhouni, R.; Eichhorn, B.; Sanchez, M.; Mazieres, M.-R.; Jaud, J. *J. Organomet. Chem.* **1995**, *490*, 21−28. [l] Wenrui, C.; Jinbi, D.; Shoushan, C. *J. Struct. Chem.* **1982**, *1*, 73−78. [m] Reference 24. [n] Gambarotta, S.; Strologo, S.; Floriani, C.; Chiesi-Villa, A.; Guastini, C. *Inorg. Chem.* **1985**, *24*, 654-660. [o] Lappert, M. F.; Raston, C. L.; Engelhardt, L. M.; White, A. H. *J. Chem. Soc., Chem. Commun.* **1985**, 521−522.

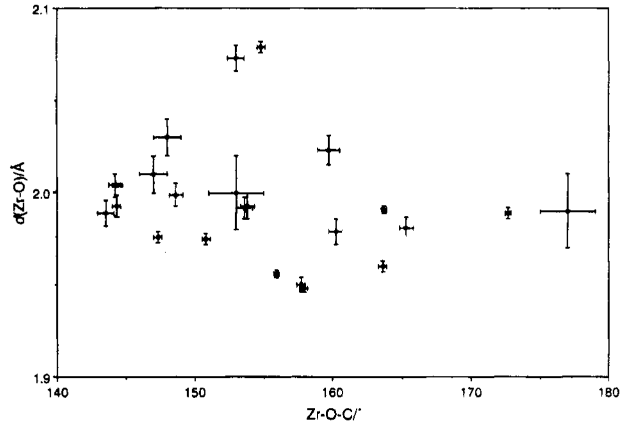

Figure 6. Correlation of Zr−O bond length and Zr−O−C bond angle for alkoxy- and aryloxyzirconocene derivatives.

bond angle in this system. For example, the Zr−OAr bond lengths in $[Cp_2Zr(OC_6H_4Cl)]_2O$ are effectively identical [1.99(2) and 2.00(2) Å], but the Zr−O−Ar bond angles vary by more than 20° [177(2)° and 153(2)°].[24] A related study by Rothwell on aryloxide derivatives of niobium and tantalum has indicated a similar lack of correlation between M−OAr distance and M−O−Ar bond angle so that it is, therefore, evident that M−O−Ar bond angles are not necessarily good indicators of M−O π-interactions.[25,26] Moreover, Cundari has noted a lack of correlation between calculated Tc═N−H bond angle and Tc═N bond length in a series of imido complexes.[27]

In view of the above evidence that M−O−Ar bond angles do not provide a good indication of the extent of M−O π-interactions, it is important to consider the origin of the linearity of the Zr−O−Ph moiety in $Cp^*_2Zr(OPh)_2$. Furthermore, since there is no low lying vacant dπ orbital orthogonal to the equatorial plane of $Cp^*_2Zr(OPh)_2$,[28] pπ−dπ overlap between O and Zr would not necessarily be expected to be promoted by expansion of the Zr−O−Ph bond angles to 180°.[29]

---

(22) The increased tendency for heavier congeners to exhibit bent structures is also observed for the pnictogens. For example, $(silox)_3TaEPh$ (silox = $(Bu^t)_3SiO$; E = N, P, As),[22a] $Cp_2Zr[P(C_6H_2(Bu^t)_3)](PMe_3)$[22b,c] and $Cp_2MP(C_6H_2(Bu^t)_3)$ (M = Mo, W)[22d,e] exhibit bent M═ER moieties. However, complexes with close to linear M═PR moieties are known, *e.g.*, $[\eta^4-N(CH_2CH_2NSiMe_3)_3]TaPCy$[22f] and $W(PMePh_2)_2(CO)Cl_2[P(2,4,6\text{-}(Bu^t)_3C_6H_2)]$.[22g] (a) Bonnano, J. B.; Wolczanski, P. T.; Lobkovsky, E. B. *J. Am. Chem. Soc.* **1994**, *116*, 11159−11160. (b) Hou, Z.; Breen, T. L.; Stephan, D. W. *Organometallics* **1993**, *12*, 3158−3167. (c) Ho, J.; Rousseau, R.; Stephan, D. W. *Organometallics* **1994**, *13*, 1918−1926. (d) Hitchcock, P. B.; Lappert, M. F.; Leung, W.-P. *J. Chem. Soc., Chem. Commun.* **1987**, 1282−1283. (e) Bohra, R.; Hitchcock, P. B.; Lappert, M. F.; Leung, W.-P. *Polyhedron* **1989**, *8*, 1884. (f) Cummins, C. C.; Schrock, R. R.; Davis, W. M. *Angew. Chem., Int. Ed. Engl.* **1993**, *32*, 756−759. (g) Cowley, A. H.; Pellerin, B.; Atwood, J. L.; Bott, S. G. *J. Am. Chem. Soc.* **1990**, *112*, 6734−6735.

(23) For a further comparison of M−OR and M−SR bonding, see: Sigel, G. A.; Power, P. P. *Inorg. Chem.* **1987**, *26*, 2819−2822.

(24) Qingchuan, Y.; Xianglin, J.; Xiaojie, X.; Genpei, L.; Youqi, T.; Shoushan, C. *Sci. Sin., Ser. B (Engl. Ed.)* **1982**, *25*, 356−366.

(25) (a) Steffey, B. D.; Fanwick, P. E.; Rothwell, I. P. *Polyhedron* **1990**, *9*, 963−968. (b) Coffindaffer, T. W.; Steffy, B. D.; Rothwell, I. P.; Folting, K.; Huffman, J. C.; Streib, W. E. *J. Am. Chem. Soc.* **1989**, *111*, 4742−4749.

(26) For a discussion of π-interactions in metal−thiolate complexes, see: (a) Ashby, M. T. *Comments Inorg. Chem.* **1990**, *10*, 297−313. (b) Wehmschulte, R. J.; Ruhlandt-Senge, K.; Power, P. P. *Inorg. Chem.* **1995**, *34*, 2593−2599.

(27) Benson, M. T.; Bryan, J. C.; Burrell, A. K.; Cundari, T. R. *Inorg. Chem.* **1995**, *34*, 2348−2355.

The near linearity of the Zr–O–Ph moiety in Cp*$_2$Zr(OPh)$_2$ also bears analogies with the linear M=N–R moieties of the 18-electron organoimido metallocene derivatives Cp*$_2$Ta(NPh)H[30,31] and Cp$_2$Zr(NBu^t)(THF).[32] Several factors, which include (i) steric interactions between the Cp* and Ph groups, (ii) π-interactions between the oxygen p-orbital and the phenyl substituent (*i.e.* Zr–O$^+$=Ph$^-$),[33] and (iii) an ionic contribution to the Zr–O bonding,[34,35] may be considered to influence the linearity of the Zr–O–Ph moiety in Cp*$_2$Zr(OPh)$_2$. However, a clear indication that steric interactions between the Cp* and phenyl groups influence the linearity of the Zr–O–Ph moiety is provided by comparison with the less sterically demanding cyclopentadienyl analogue Cp$_2$Zr(OPh)$_2$, which exhibits a greatly reduced Zr–O–Ph bond angle [147(1)°], as illustrated in Figures 1 and 2. If the dominant factor influencing the linearity of the Zr–O–Ph angle in Cp*$_2$Zr(OPh)$_2$ were a mechanism to promote electron donation to the zirconium center, one would expect the less electron rich derivative Cp$_2$Zr(OPh)$_2$ to exhibit a linear Zr–O–Ph moiety as well.[36] Such an argument, therefore, supports the notion that the linearity at oxygen in Cp*$_2$Zr(OPh)$_2$ is attributable to steric interactions.[37,38]

Another feature of interest in the structures of Cp*$_2$Zr(EPh)$_2$ centers on the conformational preferences of the phenylchalcogenolate ligands. For a given Zr–E–C bond angle, various arrangements of the phenylchalcogenolate ligands are possible, and such conformations may be conveniently classified according to the magnitude of the E–Zr–E–C torsion angle (τ), as illustrated in Figure 7. Thus, an E–M–E–C torsion angle of 0° corresponds to an endo conformation with the phenyl substituent in the E–Zr–E plane,[39] while a torsion angle of 180° corresponds to a planar exo conformation. Similarly, an E–Zr–E–C torsion angle of 90° represents a situation in which the substituents are pointed directly toward the cyclopentadienyl rings. The average torsion angle and bond angle data for Cp*$_2$Zr(EPh)$_2$ (E = O, S, Se, Te) and related group IV metallocene thiolate derivatives are summarized in Table 4. Thus, with average E–Zr–E–C torsion angles in the range 34°–58°, all of the derivatives Cp*$_2$Zr(EPh)$_2$ (E = O, S, Se, Te) exhibit an endo conformation, as illustrated in Figure 8 for Cp*$_2$Zr(SPh)$_2$. The presence of endo conformations for Cp*$_2$Zr(EPh)$_2$ is in accord with theoretical calculations on Cp$_2$M(SR)$_2$ derivatives,[28a,40] most recently performed by Hall.[41] Specifically, since the vacant metal orbital of d^0-Cp$_2$M(SR)$_2$ complexes is located lateral rather than central to the S–M–S moiety, d^0 derivatives favor an endo conformation (with R–S–M–S dihedral angles < 90°) in order to maximize pπ–dπ overlap between sulfur and the metal. In contrast, electronic factors favor an exo conformation (with S–M–S–C dihedral angles close to 180°) for d^2-Cp$_2$M(SR)$_2$ derivatives, in order to minimize destabilizing interactions between the lone pairs of electrons on sulfur and on the metal center.[42,43]

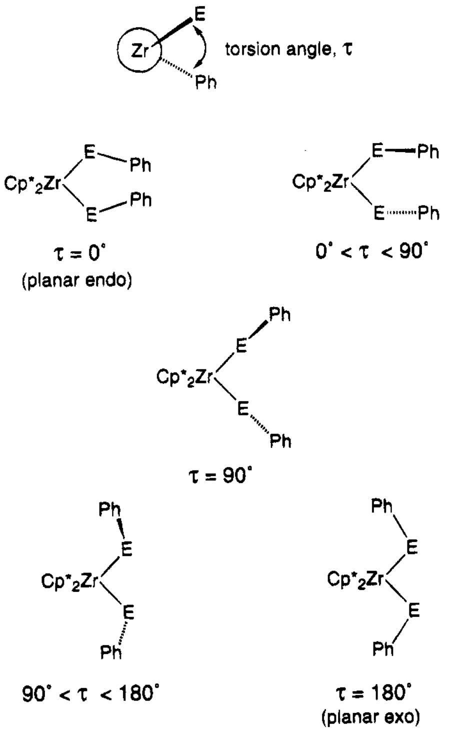

Figure 7. Possible conformations of Cp*$_2$Zr(EPh)$_2$ derivatives.

---

(28) (a) Lauher, J. W.; Hoffmann, R. *J. Am. Chem. Soc.* **1976**, *98*, 1729–1742. (b) Lin, Z.; Hall, M. B. *Coord. Chem. Rev.* **1993**, *123*, 149–167. (c) Green, J. C.; Jackson, S. E.; Higginson, B. *J. Chem. Soc., Dalton Trans.* **1975**, 403–409.

(29) It is, of course, possible that π-interactions orthogonal to the equatorial plane could occur at the expense of the Zr–Cp* interactions. For example, such interactions have been proposed for (η^5-C$_5$R$_5$)$_2$M=O (M = Mo, W)[29a] and (η^5-C$_5$R$_5$)$_2$V=NR[29b–d] complexes. (a) Bridgeman, A. J.; Davis, L.; Dixon, S. J.; Green, J. C.; Wright, I. N. *J. Chem. Soc., Dalton Trans.* **1995**, 1023–1027. (b) Osborne, J. H.; Rheingold, A. L.; Trogler, W. C. *J. Am. Chem. Soc.* **1985**, *107*, 7945–7952. (c) Gambarotta, S.; Chiesi-Villa, A.; Guastini, C. *J. Organomet. Chem.* **1984**, *270*, C49–C52. (d) Wiberg, N.; Häring, H.-W.; Schubert, U. *Z. Naturforsch.* **1980**, *35b*, 599–603.

(30) Parkin, G.; van Asselt, A.; Leahy, D. J.; Whinnery, L.; Hua, N. G.; Quan, R. W.; Henling, L. M.; Schaefer, W. P.; Santarsiero, B. D.; Bercaw, J. E. *Inorg. Chem.* **1992**, *31*, 82–85.

(31) For an analysis of the bonding in Cp*$_2$Ta(NPh)H, see: Jørgensen, K. A. *Inorg. Chem.* **1993**, *32*, 1521–1522.

(32) (a) Walsh, P. J.; Hollander, F. J.; Bergman, R. G. *J. Am. Chem. Soc.* **1988**, *110*, 8729–8731. (b) Meyer, K. E.; Walsh, P. J.; Bergman, R. G. *J. Am. Chem. Soc.* **1994**, *116*, 2669–2670.

(33) (a) Coffindaffer, T. W.; Rothwell, I. P.; Huffman, J. C. *Inorg. Chem.* **1983**, *22*, 2906–2910. (b) Watenpaugh, K.; Caughlan, C. N. *Inorg. Chem.* **1966**, *5*, 1782–1786.

(34) At the extreme of a completely ionic interaction (*i.e.*, Zr$^+$O^{2-}Ph$^+$), a linear geometry would be anticipated. See: (a) Samuels, J. A.; Lobkovsky, E. B.; Streib, W. E.; Folting, K.; Huffman, J. C.; Zwanziger, J. W.; Caulton, K. G. *J. Am. Chem. Soc.* **1993**, *115*, 5093–5104. (b) Cayton, R. H.; Chisholm, M. H.; Davidson, E. R.; DiStasi, V. F.; Du, P.; Huffman, J. C. *Inorg. Chem.* **1991**, *30*, 1020–1024.

(35) Indeed, the shortness of the Zr–O bond in these systems has been rationalized in terms of an ionic contribution, *i.e.*, Zr$^{\delta+}$–O$^{\delta-}$ (see text).

(36) Cp* ligands are more electron-donating than Cp ligands. See, for example: (a) Cauletti, C.; Green, J. C.; Kelly, M. R.; Powell, P.; Van Tilborg, J.; Robbins, J.; Smart, J. *J. Electron Spectrosc. Relat. Phenom.* **1980**, *19*, 327–353. (b) Bercaw, J. E.; Marvich, R. H.; Bell, L. G.; Brintzinger, H. H. *J. Am. Chem. Soc.* **1972**, *94*, 1219–1238. (c) Sikora, D. J.; Rausch, M. D.; Rogers, R. D.; Atwood, J. L. *J. Am. Chem. Soc.* **1981**, *103*, 1265–1267.

(37) Steric interactions, rather than an electronic preference, have recently been proposed to account for the linear [176.0(4)°] Mo–O–Me geometry in the cation *trans*-[Mo(dppe)$_2$(O)(OMe)]$^+$.[37a] Specifically, if the linear Mo–O–Me geometry were a manifestation of maximum π-donation from O to Mo, a lengthening of the *trans* Mo=O bond would be expected. However, the Mo=O bond length in *trans*-[Mo(dppe)$_2$(O)(OMe)]$^+$ [1.723(4) Å] is significantly shorter than that in the hydroxy derivative *trans*-[Mo(dppe)$_2$(O)(OH)]$^+$ [1.833(5) Å],[37b] even though the Mo–OMe and Mo–OH bond lengths are comparable. Accordingly, EHMO calculations supported the notion that the linearity of the Mo–O–Me moiety is a consequence of steric interactions between the OMe group and the phenyl groups of the dppe ligands. (a) Adachi, T.; Hughes, D. L.; Ibrahim, S. K.; Okamoto, S.; Pickett, C. J.; Yabanouchi, N.; Yoshida, T. *J. Chem. Soc., Chem. Commun.* **1995**, 1081–1083. (b) Churchill, M. R.; Rotella, F. J. *Inorg. Chem.* **1978**, *17*, 668–673.

(38) Molecular mechanics and EHMO calculations on the dimers *trans*-[Cp*Zr(SEt)$_2$(μ_2-SEt)]$_2$ and *trans*-[Cp*Zr(OMe)$_2$(μ_2-OMe)]$_2$ indicate that the planarity of the bridging O and S atoms is a consequence of steric factors, rather than π-bonding. See: Heyn, R. H.; Stephan, D. W. *Inorg. Chem.* **1995**, *34*, 2804–2812.

(39) However, for M–E–R bond angles significantly less than 180°, such planar endo conformations are not precedented due to the steric interactions that would exist between the R groups.

(40) Calhorda, M. J.; Carrondo, M. A. A. F. de C. T.; Dias, A. R.; Frazao, C. F.; Hursthouse, M. B.; Martinho Simoes, J. A.; Teixeira, C. *Inorg. Chem.* **1988**, *27*, 2513–2518.

(41) Simpson, C. Q., II; Hall, M. B. *New J. Chem.* **1991**, *15*, 763–768.

Table 4. Average Bond Angle and Torsion Angle Data for (η^5-C_5R_5)M(ER)$_2$ Derivatives (M = Ti, Zr, Hf)

	M–E–C/deg	E–M–E/deg	E–M–E–C/deg	ref
$Cp_2Ti(OPh)_2$	139	98	73	*a*
$Cp_2Ti(OC_6H_2Cl_3)_2$	141	97	109	*b*
$Cp_2Ti(SMe)_2$	110	94	57	*c, d*
$Cp_2Ti(SEt)_2$	109	94	57	*e*
$Cp_2Ti(SPh)_2$	114	99	63	*f*
$Cp_2Ti[S(CH_2)_3PPh_2]_2$	110	93	54	*g*
$Cp_2Zr(OPh)_2$	147	98	113	this work
$Cp_2Zr(OC_6F_5)_2$	164	96	136	*h*
$(\eta^5\text{-}C_5H_4Me)_2Zr(OC_6H_3Cl_2)_2$	148	105	102	*i*
$Cp^*_2Zr(OPh)_2$	173	99	34	this work
$Cp^*_2Zr(SPh)_2$	119	101	49	this work
$Cp^*_2Zr(SePh)_2$	117	100	58	this work
$Cp^*_2Zr(TePh)_2$	113	97	57	this work
$(\eta^5\text{-}C_5H_4Me)_2Hf(OC_6H_3Cl_2)_2$	148	104	104	*j*

[a] Kalirai, B. S.; Foulon, J.-D.; Hamor, T. A.; Jones, C. J.; Beer, P. D.; Fricker, S. P. *Polyhedron* **1991**, *10*, 1847–1856. [b] Reference 24. [c] Carrondo, M. A. A. F. de C. T.; Jeffrey, G. A. *Acta. Crystallogr.* **1983**, *C39*, 42–44. [d] Wark, T. A.; Stephan, D. W. *Organometallics* **1989**, *8*, 2836–2843. [e] Reference 40. [f] Muller, E. G.; Watkins, S. F.; Dahl, L. F. *J. Organomet. Chem.* **1976**, *111*, 73–89. [g] White, G. S.; Stephan, D. W. *Organometallics* **1987**, *6*, 2169–2175. [h] Amor, J. I.; Burton, N. C.; Cuenca, T.; Gómez-Sal, P.; Royo, P. *J. Organomet. Chem.* **1995**, *485*, 153–60. [i] Jinbi, D.; Meizhen, L.; Jiping, Z.; Shoushen, C. *J. Struct. Chem.* **1982**, *1*, 63–69. [j] Shiqi, D.; Shoushan, C. *Chem. J. Chin. Uni.* **1984**, *5*, 812–816.

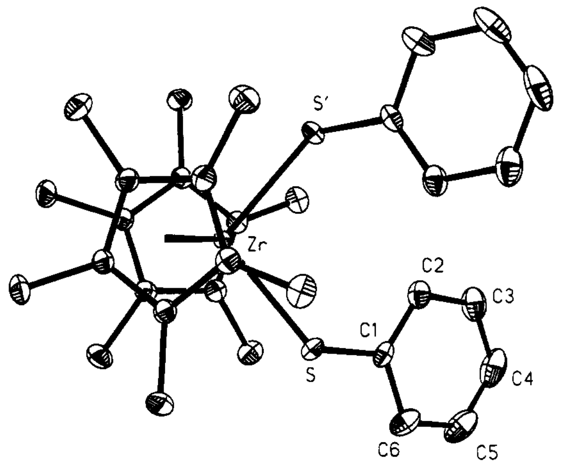

Figure 8. View of the endo conformation adopted by $Cp^*_2Zr(SPh)_2$.

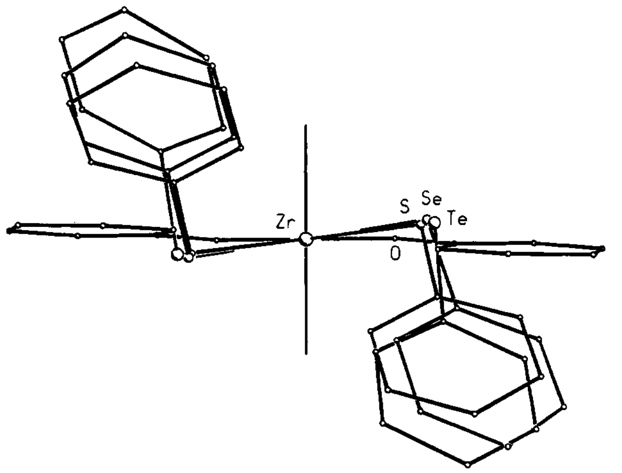

Figure 9. Variation of the E–Zr–E–C torsion angle in $Cp^*_2Zr(EPh)_2$ (E = O, S, Se, Te) as a function of the chalcogen.

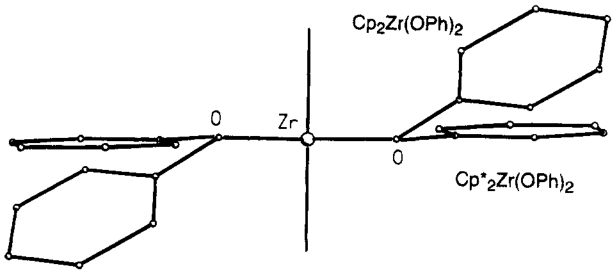

Figure 10. Variation of the O–Zr–O–C torsion angle in $Cp_2Zr(OPh)_2$ and $Cp^*_2Zr(OPh)_2$.

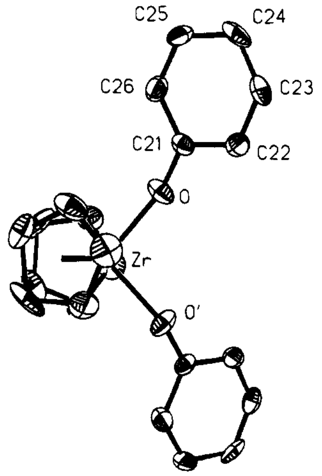

Figure 11. View of the (slight) exo conformation adopted by $Cp_2Zr(OPh)_2$.

The magnitude of the displacement of the phenyl substituents from the equatorial plane is reflected by the E–Zr–E–C torsion angle and, as expected, is coupled to the Zr–E–Ph bond angle. Therefore, the displacement is least for the oxo derivative, which exhibits the largest Zr–E–Ph bond angle. The conformational variation for the series $Cp^*_2Zr(EPh)_2$ (E = O, S, Se, Te) is illustrated in Figure 9. Moreover, compared with $Cp^*_2Zr(OPh)_2$, the zirconocene analogue $Cp_2Zr(OPh)_2$ exhibits a O–Zr–O–C torsion angle (113°) that is much closer to 90°, so that the phenyl substituents of the latter are pointed more directly toward the cyclopentadienyl groups (Figure 10). Interestingly, the O–Zr–O–C torsion angle in $Cp_2Zr(OPh)_2$ is greater than 90°, so that there is a slight preference for anexo, rather than endo, conformation (Figure 11). Large O–M–O–C torsion angles (*i.e.* >90°) have also been reported for other zirconocene aryloxy derivatives (Table 4).

Summary

In summary, $Cp^*_2Zr(EPh)_2$ (E = O, S, Se, Te) represent the first complete series of phenylchalcogenolate complexes to be

---

(42) For d^1- and d^2-derivatives, conformations with torsion angles of 0° (endo) and 180° (exo) are effectively equally favored on electronic grounds alone. However, steric interactions between the R substituents in the endo conformation prohibit coplanarity of the R–S–M–S–R moiety so that complexes with R–S–M–S dihedral angles of 0° have not been observed (see ref 41).

Table 5. ^{1}H and ^{13}C NMR Data for $Cp^*_2Zr(EPh)_2$ (E = S, Se, Te)

	$Cp^*_2Zr(SPh)_2$	$Cp^*_2Zr(SePh)_2$	$Cp^*_2Zr(TePh)_2$
		^{1}H NMR (C_6D_6)	
η^5-$C_5(CH_3)_5$	1.86 [s]	1.89 [s]	1.91 [s]
E−C_6H_5			
ortho	7.84 [m]	8.02 [m]	8.26 [m]
meta	6.96 [m]	6.95 [m]	6.98 [m]
para	6.88 [m]	6.95 [m]	6.98 [m]
		^{13}C NMR (C_6D_6)	
η^5-$C_5(CH_3)_5$	12.3 [q, $^1J_{C-H} = 127$]	12.7 [q, $^1J_{C-H} = 127$]	13.6 [q, $^1J_{C-H} = 127$]
η^5-$C_5(CH_3)_5$	122.0 [s]	121.7 [s]	121.2 [s]
E−C_6H_5			
ipso	143.0 [t, $^2J_{C-H} = 8$]	135.2[a]	112.5 [t, $^2J_{C-H} = 7$]
ortho	128.0 [dd, $^1J_{C-H} = 158$, $^2J_{C-H} = 8$]	128.3 [dd, $^1J_{C-H} = 158$, $^2J_{C-H} = 7$]	128.8 [dd, $^1J_{C-H} = 159$, $^2J_{C-H} = 7$]
meta	134.0 [dt, $^1J_{C-H} = 160$, $^2J_{C-H} = 7$]	136.4 [dt, $^1J_{C-H} = 162$, $^2J_{C-H} = 6$]	141.9 [dt, $^1J_{C-H} = 162$, $^2J_{C-H} = 7$]
para	124.6 [dt, $^1J_{C-H} = 160$, $^2J_{C-H} = 7$]	125.3 [dt, $^1J_{C-H} = 159$, $^2J_{C-H} = 8$]	126.1 [dt, $^1J_{C-H} = 160$, $^2J_{C-H} = 7$]

[a] $^2J_{C-H}$ is obscured by resonance at 136.4 ppm.

structurally characterized by X-ray diffraction.[44] Although the Zr−SPh, Zr−SePh, and Zr−TePh bond lengths in $Cp^*_2Zr(EPh)_2$ are comparable to the values predicted by the sum of the respective covalent radii, the Zr−O bond length in $Cp^*_2Zr(OPh)_2$ is substantially shorter than the sum of its covalent radii. A similar observation has been made previously for the terminal chalcogenido complexes $(\eta^5\text{-}C_5Me_4Et)_2Zr(E)(NC_5H_5)$, for which the Zr=O bond length is shorter than would be predicted by comparison with the other derivatives. The shortening of both the Zr−OPh and Zr=O bonds in these systems may be attributed to an ionic contribution to the bonding. Ionic contributions are expected to be less significant for the less electronegative and larger chalcogens, so that the Zr−SPh, Zr−SePh, and Zr−TePh bond lengths compare well with the sum of the respective covalent radii. Finally, another interesting difference in the structures of $Cp^*_2Zr(EPh)_2$ (E = O, S, Se, Te) is the near linearity [172.7(2)°] of the Zr−O−Ph moiety compared with the bent structures [113°−119°] observed for Zr−E−Ph (E = S, Se, Te). However, since the cyclopentadienyl analogue $Cp_2Zr(OPh)_2$ exhibits a bent Zr−O−Ph moiety [147(1)°], it is proposed that steric interactions between the Cp* and phenyl groups are mainly responsible for enforcing linearity in $Cp^*_2Zr(OPh)_2$. Thus, short M−OR bond lengths and linear M−O−R moieties are not necessarily a consequence of a strong $p\pi-d\pi$ lone pair donation from oxygen to the metal.

Experimental Details

1. General Considerations. All manipulations were performed using a combination of glovebox, high-vacuum, or Schlenk techniques. Solvents were purified and degassed by standard procedures. ^{1}H and ^{13}C NMR spectra were measured on Varian VXR 200, 300, and 400 spectrometers in C_6D_6. ^{1}H and ^{13}C chemical shifts are reported in parts per million relative to $SiMe_4$ ($\delta = 0$) and were referenced internally with respect to the protio solvent impurity ($\delta = 7.15$ for C_6D_5H) or the ^{13}C resonances ($\delta = 128.0$ for C_6D_6), respectively. ^{77}Se and ^{125}Te NMR spectra were recorded on a Varian VXR 300 spectrometer operating at 57.2 and 94.6 MHz, respectively. ^{77}Se chemical shifts are reported in parts per million relative to neat Me_2Se ($\delta = 0$) and were referenced using a solution of Ph_2Se_2 in C_6D_6 ($\delta = 460$) as external standard.[45] ^{125}Te chemical shifts are reported in parts per million relative to neat Me_2Te ($\delta = 0$) and were referenced using either a solution of Ph_2Te_2 in $CDCl_3$ ($\delta = 420.8$ ppm)[46] or a solution of $Te(OH)_6$ (1.74 M in D_2O, $\delta = 712$ ppm)[14,47] as external standards. Coupling constants are reported in hertz. IR spectra were recorded as KBr pellets on a Perkin-Elmer 1600 FTIR spectrophotometer, and the data are reported in cm^{-1}. Elemental analyses were determined using a Perkin-Elmer 2400 CHN analyzer. $Cp_2Zr(CO)_2$,[48] Cp_2ZrMe_2,[49] and $Cp^*_2Zr(CO)_2$[48] were prepared by literature methods.

2. Synthesis of $Cp_2Zr(OPh)_2$. A mixture of Cp_2ZrMe_2 (0.30 g, 1.2 mmol) and PhOH (0.22 g, 2.4 mmol) in toluene (5 mL) was stirred at room temperature for 1.5 days. The volatile components were removed, and the residue was washed with pentane (10 mL) and dried in vacuo to give $Cp_2Zr(OPh)_2$ (0.39 g, 80% yield) as a white solid. Anal. Calcd for $C_{22}H_{20}O_2Zr$: C, 64.8%; H, 5.0%. Found: C, 64.8%; H, 4.7%. IR data: 3073 (m), 3015 (w), 1587 (vs), 1481 (vs), 1271 (vs), 1161 (s), 1066 (m), 1015 (m), 870 (vs), 803 (vs), 756 (vs), 694 (s), 613 (s), 518 (w), 436 (w). ^{1}H NMR (C_6D_6): 5.94 [10H, s, 2(η^5-C_5H_5)], 6.77 [4H, d, $^3J_{H-H} = 8$, 2(*o*-OPh)], 6.89 [2H, t, $^3J_{H-H} = 7$, 2(*p*-OPh)], 7.25 [4H, t, $^3J_{H-H} = 8$, 2(*m*-OPh)]. ^{13}C NMR (C_6D_6): 113.3 [d of multiplet, $^1J_{C-H} = 173$, 2(η^5-C_5H_5)], 118.6 [d, $^1J_{C-H} = 156$, 2(*m*-OPh)], 119.6 [dt, $^1J_{C-H} = 159$, $^2J_{C-H} = 7$, 2(*p*-OPh)], 129.8 [dd, $^1J_{C-H} = 156$, $^2J_{C-H} = 9$, 2(*o*-OPh)], 166.1 [t, $^2J_{C-H} = 8$, 2(*ipso*-OPh)].

3. Synthesis of $Cp^*_2Zr(OPh)_2$. A mixture of $Cp^*_2Zr(CO)_2$ (0.20 g, 0.48 mmol) and PhOH (0.09 g, 0.96 mmol) in toluene (3 mL) was stirred at 85 °C for 2.5 days. The volatile components were removed, and the residue was washed with pentane (3 mL) and dried in vacuo to give $Cp^*_2Zr(OPh)_2$ as a white solid (0.21 g, 78%). The product was identified by comparison of its ^{1}H NMR data with that of an authentic sample.[6]

4. Synthesis of $Cp^*_2Zr(SPh)_2$. A mixture of $Cp^*_2Zr(CO)_2$ (0.10 g, 0.24 mmol) and Ph_2S_2 (0.05 g, 0.24 mmol) in toluene (4 mL) was stirred at 55 °C for 2 days giving a yellow solution. The volatile components were removed, and the residue was washed with pentane (5 mL) and dried *in vacuo* to give $Cp^*_2Zr(SPh)_2$ (0.11 g) as a yellow solid. A further quantity of $Cp^*_2Zr(SPh)_2$ (0.01 g) was obtained by crystallization of the solution resulting from the pentane wash; total yield of $Cp^*_2Zr(SPh)_2$, 0.12 g, 87%. Anal. Calcd for $C_{32}H_{40}S_2Zr$: C, 66.3%; H, 7.0%. Found: C, 66.6%; H, 7.1%. IR data: 3057 (m), 2986 (s), 2902 (vs), 1576 (s), 1473 (vs), 1438 (vs), 1376 (m), 1082 (m), 1024 (vs), 738 (vs), 695 (vs), 595 (w), 483 (w), 437 (w), 400 (w). ^{1}H and ^{13}C NMR data are listed in Table 5.

5. Synthesis of $Cp^*_2Zr(SePh)_2$. A mixture of $Cp^*_2Zr(CO)_2$ (0.10 g, 0.24 mmol) and Ph_2Se_2 (0.08 g, 0.24 mmol) in toluene (5 mL) was

---

(43) For some recent experimental studies on the conformations of arylthiolate ligands in $Cp_2Nb(S\text{-}p\text{-}C_6H_4X)_2$ and $[Cp_2Nb(S\text{-}p\text{-}C_6H_4X)_2]^+$, see: Darensbourg, M. Y.; Bischoff, C. J.; Houliston, S. A.; Pala, M.; Reibenspies, J. *J. Am. Chem. Soc.* **1990**, *112*, 6905−6912.

(44) The structures of $[Ph_4P][Mn(SPh)_4]$,[44a] $[Et_4N][Mn(SePh)_4]$,[44b] and $[Et_4N][Mn(TePh)_4]$,[44b] but not that of the phenoxy derivative, have been determined previously. (a) Swenson, D.; Baenziger, N. C.; Coucouvanis, D. *J. Am. Chem. Soc.* **1978**, *100*, 1932−1934. (b) Tremel, W.; Krebs, B.; Greiwe, K.; Simon, W.; Stephan, H.-O.; Henkel, G. *Z. Naturforsch.* **1992**, *47b*, 1580−1592.

(45) Lardon, M. *J. Am. Chem. Soc.* **1970**, *92*, 5063−5066.

(46) Granger, P.; Chapelle, S.; McWhinnie, W. R.; Al-Rubaie, A. *J. Organomet. Chem.* **1981**, *220*, 149−158.

(47) The ^{125}Te NMR signal for aqueous $Te(OH)_6$ has also been reported to be 707 ppm.[47a] However, we find better internal consistency by adopting the value of 712 ppm for this reference. (a) Tötsch, W.; Peringer, P.; Sladky, F. *J. Chem. Soc., Chem. Commun.* **1981**, 841−842.

(48) Sikora, D. J.; Moriarty, K. J.; Rausch, M. D. *Inorg. Synth.* **1990**, *28*, 248−257.

(49) Samuel, E.; Rausch, M. D. *J. Am. Chem. Soc.* **1973**, *95*, 6263−6267.

Table 6. Crystal and Intensity Collection Data for $Cp_2Zr(OPh)_2$ and $Cp^*{}_2Zr(EPh)_2$ (E = O, S, Se, Te)

	$Cp_2Zr(OPh)_2$	$Cp^*{}_2Zr(OPh)_2$	$Cp^*{}_2Zr(SPh)_2$	$Cp^*{}_2Zr(SePh)_2$	$Cp^*{}_2Z(TePh)_2$
formula	$C_{22}H_{20}O_2Zr$	$C_{32}H_{40}O_2Zr$	$C_{32}H_{40}S_2Zr$	$C_{32}H_{40}Se_2Zr$	$C_{32}H_{40}Te_2Zr$
formula weight	407.6	547.9	580.0	673.8	771.1
lattice	orthorhombic	monoclinic	monoclinic	hexagonal	monoclinic
cell constants					
a, Å	8.274(3)	11.049(2)	14.444(4)	12.903(2)	16.917(3)
b, Å	19.843(9)	15.445(3)	11.449(2)	12.903(2)	25.326(6)
c, Å	11.586(8)	17.141(3)	18.262(3)	31.923(6)	15.234(4)
α, deg	90.0	90.0	90.0	90.0	90.0
β, deg	90.0	104.24(1)	103.39(2)	90.0	107.95(2)
γ, deg	90.0	90.0	90.0	120.0	90.0
V, $Å^3$	1902(1)	2835(1)	2921(2)	4603(2)	6212(3)
Z	4	4	4	6	8
radiation (λ, Å)	Mo Kα (0.71073)	Mo Kα (0.71073)	Mo Kα (0.71073)	Mo Kα (0.71073)	Mo Kα (0.71073)
space group	*Aba*2 (No. 41)	*C*2/*c* (No. 15)	*C*2/*c* (No. 15)	$P6_1$ (No. 169)	$P2_1/c$ (No. 14)
ρ(calcd), g cm^{-3}	1.423	1.290	1.319	1.458	1.649
μ(Mo Kα), cm^{-1}	5.89	4.10	5.38	27.48	22.13
R^a	0.0626	0.0374	0.0306	0.0532	0.0321
$R_w{}^a$	0.0660	0.0472	0.0445	0.0557	0.0437

[a] $R = \sum|F_o - F_c|\}/\sum|F_o|$; $R_w = \sum w^{1/2}|F_o - F_c|/\sum w^{1/2}|F_o|$; $w = [\sigma^2(F) + gF^2]^{-1}$.

Table 7. Atomic Coordinates ($\times 10^4$) and Temperature Factors ($Å^2 \times 10^3$) for $Cp_2Zr(OPh)_2$

	x	*y*	*z*	*U*(eq)[a]
Zr	0	0	2247	49(1)
O	1354(13)	−515(4)	3383(16)	79(4)
C(11)	753(28)	812(12)	718(24)	100(9)
C(12)	772(29)	1189(10)	1694(28)	100(9)
C(13)	1903(25)	997(10)	2337(35)	101(8)
C(14)	2749(22)	510(11)	1895(22)	95(10)
C(15)	2173(35)	347(10)	812(28)	121(11)
C(21)	1720(18)	−1110(6)	3823(19)	58(5)
C(22)	1039(18)	−1354(7)	4843(20)	67(6)
C(23)	1515(26)	−1969(9)	5251(21)	72(7)
C(24)	2673(34)	−2343(7)	4834(40)	84(8)
C(25)	3373(28)	−2106(12)	3796(22)	91(9)
C(26)	2933(20)	−1505(8)	3336(20)	77(6)

[a] Equivalent isotropic *U* defined as one-third of the trace of the orthogonalized $\mathbf{U}_{ij}$ tensor.

stirred for 17 h at room temperature. The volatile components were removed to give an orange oily solid which was washed with pentane (5 mL) and dried *in vacuo* to give $Cp^*{}_2Zr(SePh)_2$ (0.10 g) as a bright orange solid. A second crop was crystallized from the pentane washings (0.04 g); total yield of $Cp^*{}_2Zr(SePh)_2$, 0.14 g. (88%). Anal. Calcd for $C_{32}H_{40}Se_2Zr$: C, 57.0%; H, 6.0%. Found: C, 57.0%; H, 6.3%. IR data: 3045 (m), 2989 (m), 2899 (vs), 1574 (s), 1473 (vs), 1447 (vs), 1378 (s), 1067 (m), 1022 (vs), 738 (vs), 694 (s), 667 (m), 598 (w), 470 (w). ^1H and ^{13}C NMR data are listed in Table 5. ^{77}Se NMR (C_6D_6): 710 [s].

6. Synthesis of $Cp^*{}_2Zr(TePh)_2$. A mixture of $Cp^*{}_2Zr(CO)_2$ (0.10 g, 0.24 mmol) and Ph_2Te_2 (0.10 g, 0.24 mmol) in toluene (5 mL) was stirred for 17 h at room temperature. The volatile components were removed to give a red-violet oily residue which was washed with pentane (5 mL) and dried *in vacuo* to yield $Cp^*{}_2Zr(TePh)_2$ (0.13 g) as a red solid. A second crop of the product was crystallized from the pentane washings (0.02 g); total yield of $Cp^*{}_2Zr(TePh)_2$, 0.15 g (78%). Anal. Calcd for $C_{32}H_{40}Te_2Zr$: C, 49.9%; H, 5.2%. Found: C, 50.2%; H, 5.3%. IR data: 3041 (m), 2984 (m), 2896 (vs), 1570 (s), 1469 (vs), 1430 (vs), 1377 (s), 1020 (vs), 731 (vs), 693 (s). ^1H and ^{13}C NMR data are listed in Table 5. ^{125}Te NMR (C_6D_6): 1004 [s].

7. Synthesis of $Cp_2Zr(SePh)_2$. A mixture of $Cp_2Zr(CO)_2$ (40 mg, 0.15 mmol) and Ph_2Se_2 (50 mg, 0.16 mmol) in benzene-d_6 (1 mL) produced $Cp_2Zr(SePh)_2$ quantitatively over 30 min at room temperature. $Cp_2Zr(SePh)_2$ has been synthesized previously[9] and was identified by ^1H NMR spectroscopy and mass spectroscopy.

8. Synthesis of $Cp_2Zr(TePh)_2$. A mixture of $Cp_2Zr(CO)_2$ (40 mg, 0.15 mmol) and Ph_2Te_2 (60 mg, 0.15 mmol) in benzene-d_6 (1 mL) produced $Cp_2Zr(TePh)_2$ quantitatively over 30 min at room temperature. $Cp_2Zr(TePh)_2$ has been synthesized previously[9] and was identified by ^1H NMR spectroscopy and mass spectroscopy.

Table 8. Atomic Coordinates ($\times 10^4$) and Temperature Factors ($Å^2 \times 10^3$) for $Cp^*{}_2Zr(OPh)_2$

	x	*y*	*z*	*U*[a]
Zr	0	6070(1)	7500	38(1)
C(11)	−2180(3)	6194(2)	6576(3)	85(2)
C(12)	−2373(3)	5935(3)	7308(3)	84(2)
C(13)	−1897(3)	5110(3)	7475(2)	73(1)
C(14)	−1444(3)	4839(2)	6818(2)	68(1)
C(15)	−1611(3)	5514(3)	6275(2)	73(1)
C(21)	−2602(5)	7051(4)	6176(5)	228(5)
C(22)	−3053(5)	6427(5)	7823(5)	219(5)
C(23)	−2073(6)	4553(5)	8163(3)	184(4)
C(24)	−1148(5)	3928(3)	6625(5)	170(4)
C(25)	−1362(6)	5501(6)	5452(3)	181(4)
O	−367(2)	6903(2)	8297(1)	74(1)
C(1)	−504(3)	7527(2)	8806(2)	57(1)
C(2)	−829(4)	7337(3)	9515(2)	71(1)
C(3)	−977(4)	7980(3)	10037(2)	89(2)
C(4)	−811(4)	8822(3)	9859(3)	100(2)
C(5)	−515(6)	9030(3)	9156(4)	110(3)
C(6)	−343(4)	8385(3)	8628(3)	82(2)

[a] Equivalent isotropic *U* defined as one-third of the trace of the orthogonalized $\mathbf{U}_{ij}$ tensor.

9. X-ray Structure Determination of $Cp_2Zr(OPh)_2$. Crystal data, data collection, and refinement parameters for $Cp_2Zr(OPh)_2$ are summarized in Table 6. A single crystal of $Cp_2Zr(OPh)_2$ was mounted in a glass capillary and placed on a Nicolet R3m diffractometer. The unit cell was determined by the automatic indexing of 25 centered reflections and confirmed by examination of the axial photographs. Intensity data were collected using graphite monochromated Mo Kα X-radiation (λ=0.71073 Å). Check reflections were measured every 100 reflections, and the data were scaled accordingly and corrected for Lorentz, polarization, and absorption effects. The structure was solved using direct methods and standard difference map techniques using SHELXTL PC. Systematic absences were consistent with the space groups *Aba*2 (No. 41) and *Acam* (No. 64), of which the noncentrosymmetric alternative *Aba*2 (No. 41) was selected and confirmed by the absence of a mirror plane in the molecule. Hydrogen atoms were included in calculated positions. Inversion of configuration indicated the correct absolute structure. Atomic coordinates are listed in Table 7.

10. X-ray Structure Determination of $Cp^*{}_2Zr(OPh)_2$. Crystal data, data collection, and refinement parameters are summarized in Table 6, and the general procedure is as described for $Cp_2Zr(OPh)_2$. Systematic absences were consistent with the space groups *Cc* (No. 9) and *C*2/*c* (No. 15), but successful solution was obtained in the centrosymmetric alternative *C*2/*c* (No. 15). Atomic coordinates are listed in Table 8.

11. X-ray Structure Determination of $Cp^*{}_2Zr(SPh)_2$. Crystal data, data collection, and refinement parameters are summarized in Table 6, and the general procedure is as described for $Cp_2Zr(OPh)_2$.

Table 9. Atomic Coordinates ($\times 10^4$) and Temperature Factors ($Å^2 \times 10^3$) for $Cp^*_2Zr(SPh)_2$

	x	*y*	*z*	*U*(eq)[a]
Zr	5000	916(1)	2500	27(1)
S	6324(1)	2319(1)	3052(1)	39(1)
C(1)	6093(2)	3477(2)	3630(2)	41(1)
C(2)	5234(3)	4082(3)	3483(2)	51(1)
C(3)	5133(3)	5060(3)	3909(2)	72(2)
C(4)	5851(4)	5426(4)	4474(3)	89(2)
C(5)	6688(4)	4837(4)	4625(3)	90(2)
C(6)	6824(3)	3850(3)	4203(2)	67(1)
C(11)	3609(2)	170(2)	3022(2)	40(1)
C(12)	4016(2)	1078(2)	3526(2)	38(1)
C(13)	4941(2)	730(2)	3897(2)	41(1)
C(14)	5111(2)	−400(3)	3628(2)	43(1)
C(15)	4263(2)	−758(2)	3106(2)	42(1)
C(21)	2587(2)	119(3)	2586(2)	54(1)
C(22)	3475(2)	2101(3)	3729(2)	52(1)
C(23)	5580(3)	1305(3)	4564(2)	54(1)
C(24)	5964(3)	−1135(3)	3969(2)	60(1)
C(25)	4011(2)	−1997(3)	2858(2)	61(1)

[a] Equivalent isotropic *U* defined as one-third of the trace of the orthogonalized $\mathbf{U}_{ij}$ tensor.

Table 10. Atomic Coordinates ($\times 10^4$) and Temperature Factors ($Å^2 \times 10^3$) for $Cp^*_2Zr(SePh)_2$

	x	*y*	*z*	*U*(eq)[a]
Zr	3604(1)	6962(1)	2500	32(1)
Se(1)	3392(2)	5124(2)	2941(2)	42(1)
Se(2)	5302(2)	7233(2)	1971(2)	47(1)
C(11)	3451(17)	8389(16)	3030(8)	56(11)
C(12)	4420(18)	9122(14)	2777(8)	53(11)
C(13)	5357(17)	8821(16)	2852(8)	51(11)
C(14)	4942(16)	7929(16)	3151(8)	49(5)
C(15)	3762(18)	7638(16)	3260(7)	59(12)
C(21)	1439(15)	6216(18)	2307(7)	47(11)
C(22)	2110(16)	7272(16)	2071(8)	55(11)
C(23)	2780(14)	7048(15)	1789(7)	50(10)
C(24)	2521(15)	5858(14)	1795(7)	32(10)
C(25)	1657(14)	5329(15)	2146(7)	40(10)
C(31)	2475(26)	8597(23)	3145(9)	115(22)
C(32)	4641(20)	10157(16)	2519(8)	79(13)
C(33)	6579(16)	9552(15)	2730(9)	79(13)
C(34)	5674(23)	7560(18)	3404(7)	77(15)
C(35)	3060(21)	6914(20)	3645(9)	91(8)
C(41)	424(18)	5903(23)	2597(9)	91(16)
C(42)	1869(17)	8289(19)	2048(8)	67(13)
C(43)	3461(17)	7867(16)	1416(8)	62(6)
C(44)	2784(15)	5153(16)	1507(7)	50(5)
C(45)	903(15)	4020(13)	2254(7)	53(10)
C(51)	3044(14)	3720(14)	2637(7)	38(10)
C(52)	3719(16)	3771(16)	2281(8)	50(11)
C(53)	3439(21)	2689(22)	2084(8)	65(15)
C(54)	2597(26)	1629(19)	2244(11)	84(18)
C(55)	1985(22)	1613(20)	2582(9)	66(15)
C(56)	2179(17)	2630(14)	2794(8)	54(10)
C(61)	6830(15)	7553(18)	2204(7)	47(11)
C(62)	6861(18)	6763(17)	2503(8)	53(12)
C(63)	7938(19)	7018(20)	2657(8)	61(14)
C(64)	8987(17)	8005(20)	2508(9)	70(14)
C(65)	8931(17)	8693(22)	2208(9)	75(14)
C(66)	7886(13)	8505(15)	2048(7)	40(10)

[a] Equivalent isotropic *U* defined as one-third of the trace of the orthogonalized $\mathbf{U}_{ij}$ tensor.

Systematic absences were consistent with the space groups *Cc* (No. 9) and *C*2/*c* (No. 15), but successful solution was obtained in the centrosymmetric alternative *C*2/*c* (No. 15).. Atomic coordinates are listed in Table 9.

Table 11. Atomic Coordinates ($\times 10^4$) and Temperature Factors ($Å^2 \times 10^3$) for $Cp^*_2Zr(TePh)_2$

	x	*y*	*z*	*U*(eq)[a]
Zr(1)	4796(1)	8728(1)	2337(1)	38(1)
Zr(2)	−1082(1)	6467(1)	3877(1)	41(1)
Te(11)	3214(1)	9048(1)	2483(1)	55(1)
Te(12)	5038(1)	7834(1)	3551(1)	61(1)
Te(21)	569(1)	6135(1)	3992(1)	61(1)
Te(22)	−1187(1)	7341(1)	2635(1)	63(1)
C(11)	3981(5)	8842(3)	626(5)	55(3)
C(12)	4821(5)	8795(3)	688(5)	51(3)
C(13)	5092(4)	8284(3)	999(4)	45(3)
C(14)	4415(4)	8003(3)	1083(4)	46(3)
C(15)	3725(4)	8340(4)	856(5)	57(3)
C(21)	5699(4)	9111(3)	3914(5)	48(3)
C(22)	6248(4)	8894(3)	3471(5)	56(3)
C(23)	6198(4)	9196(3)	2683(5)	55(3)
C(24)	5578(5)	9592(3)	2594(5)	55(3)
C(25)	5289(4)	9537(3)	3373(5)	50(3)
C(31)	3409(6)	9281(4)	195(6)	101(5)
C(32)	5260(7)	9180(3)	225(6)	93(5)
C(33)	5913(5)	8038(3)	1043(6)	75(4)
C(34)	4387(6)	7413(3)	1160(6)	88(5)
C(35)	2830(5)	8166(5)	665(6)	105(5)
C(41)	5669(5)	8982(3)	4858(5)	70(4)
C(42)	6912(5)	8494(3)	3883(6)	79(4)
C(43)	6868(5)	9190(4)	2219(7)	95(5)
C(44)	5404(6)	10061(3)	1978(6)	88(5)
C(45)	4805(5)	9960(3)	3667(5)	66(4)
C(51)	−366(6)	6419(3)	5619(5)	67(4)
C(52)	−159(5)	6926(3)	5370(5)	53(3)
C(53)	−878(5)	7210(3)	5075(5)	48(3)
C(54)	−1547(4)	6904(3)	5110(5)	52(3)
C(55)	−1231(6)	6410(3)	5477(5)	65(4)
C(61)	−2490(4)	6285(3)	2656(5)	57(3)
C(62)	−1885(4)	6069(3)	2276(5)	50(3)
C(63)	−1501(4)	5650(3)	2832(5)	52(3)
C(64)	−1835(5)	5592(3)	3563(5)	58(3)
C(65)	−2478(5)	5971(3)	3434(5)	57(3)
C(71)	242(7)	6009(5)	6139(6)	133(6)
C(72)	711(5)	7145(4)	5612(7)	105(5)
C(73)	−942(6)	7793(3)	4927(6)	80(4)
C(74)	−2405(5)	7113(4)	4996(6)	96(5)
C(75)	−1643(7)	6005(4)	5926(6)	106(5)
C(81)	−3145(5)	6682(3)	2215(6)	80(4)
C(82)	−1824(5)	6195(3)	1336(5)	71(4)
C(83)	−963(5)	5227(3)	2586(6)	72(4)
C(84)	−1651(6)	5124(3)	4229(5)	80(4)
C(85)	−3170(5)	5946(4)	3852(6)	90(5)
C(91)	3227(4)	9208(3)	3865(5)	51(3)
C(92)	3425(5)	8824(3)	4528(6)	67(4)
C(93)	3323(5)	8919(4)	5373(6)	76(4)
C(94)	3046(5)	9394(4)	5581(6)	74(4)
C(95)	2835(5)	9774(3)	4928(6)	69(4)
C(96)	2921(4)	9686(3)	4069(5)	56(3)
C(101)	4016(5)	7307(3)	3177(5)	58(4)
C(102)	4167(6)	6762(3)	3216(6)	76(4)
C(103)	3520(8)	6418(4)	3017(7)	91(5)
C(104)	2735(7)	6575(4)	2793(7)	88(5)
C(105)	2582(6)	7111(4)	2760(7)	93(5)
C(106)	3222(6)	7463(3)	2962(7)	78(5)
C(111)	695(4)	5906(3)	2698(5)	54(3)
C(112)	1092(5)	5430(3)	2641(6)	76(4)
C(113)	1205(6)	5290(4)	1819(7)	90(5)
C(114)	948(6)	5609(5)	1069(7)	105(6)
C(115)	590(6)	6080(4)	1136(6)	95(5)
C(116)	459(5)	6232(3)	1952(6)	70(4)
C(121)	−224(6)	7893(3)	3145(5)	65(4)
C(122)	596(7)	7749(4)	3361(6)	83(5)
C(123)	1217(6)	8128(5)	3659(7)	97(5)
C(124)	1033(7)	8642(4)	3737(7)	89(5)
C(125)	234(8)	8791(3)	3532(6)	80(5)
C(126)	−405(6)	8425(3)	3214(5)	68(4)

[a] Equivalent isotropic *U* defined as one-third of the trace of the orthogonalized $\mathbf{U}_{ij}$ tensor.

12. X-ray Structure Determination of $Cp^*_2Zr(SePh)_2$. Crystal data, data collection, and refinement parameters are summarized in Table 6, and the general procedure is as described for $Cp_2Zr(OPh)_2$. Systematic absences for $Cp^*_2Zr(SePh)_2$ were consistent with the pairs of space groups {$P6_1$ (No. 169) and $P6_5$ (No. 170)}, and {$P6_122$ (No. 178) and $P6_522$ (No. 179)}. R_{int} strongly suggested the options $P6_1$ (No. 169) and $P6_5$ (No. 170) and were confirmed by the success of the solution. A satisfactory solution could not be obtained for the space groups $P6_122$ (No. 178) and $P6_522$ (No. 179). Inversion of configuration established the correct choice of enantiomorph and space group as $P6_1$ (No. 169). Atomic coordinates are listed in Table 10.

13. X-ray Structure Determination of $Cp^*_2Zr(TePh)_2$. Crystal data, data collection, and refinement parameters are summarized in Table 6, and the general procedure is as described for $Cp_2Zr(OPh)_2$. Systematic absences were consistent uniquely with the space group $P2_1/c$ (No. 14). Atomic coordinates are listed in Table 11.

Acknowledgment. We thank the U. S. Department of Energy, Office of Basic Energy Sciences (Grant No. DE-FG02-93ER14339), and the donors of the Petroleum Research Fund, administered by the ACS, for partial support of this research. G.P. is the recipient of a Camille and Henry Dreyfus Teacher-Scholar Award (1991–1996) and a Presidential Faculty Fellowship Award (1992–1997). T.M.T. acknowledges the Camille and Henry Dreyfus Foundation for the Jean Dreyfus Boissevain Undergraduate Scholarship in Chemistry (1994–1995).

Supporting Information Available: Tables S1–S30 of crystal and intensity collection data, atomic coordinates, bond distances and angles, and anisotropic displacement parameters and figures of ORTEP diagrams for $Cp_2Zr(OPh)_2$ and $Cp^*_2Zr(EPh)_2$ (E = O, S, Se, Te) (39 pages). This material is contained in many libraries on microfiche, immediately follows this article in the microfilm version of the journal, and can be ordered from the ACS; see any current masthead page for ordering information.

IC950607U